Massive stars in Carina from GES, GOSSS & LiLiMaRlin

A new census of OB stars to obtain a reliable distribution of rotational velocities for the O-star population

S. R. Berlanas[1,2], J. Maíz Apellániz[3], A. Herrero[4,5] et al.

1. UA, Alicante, Spain. 2. Keele University, UK. 3. CAB, Madrid, Spain. 4. IAC, Tenerife, Spain. 5. ULL, Tenerife, Spain.

The Carina Nebula complex consists on several stellar groups, some bound and some not, immersed in the Car OB1 association, a unique region to study Galactic massive stars. Containing a large number of O-stars, it is the most massive star-forming region within 3 kpc of the Sun. Even though the Carina nebula harbors hundreds of massive stars, there is no systematic spectroscopic analysis of its early-type members.

In this contribution we present results from *Berlanas et al. 2022 (in prep*) in which we created the most complete to date census of massive stars in the central part of the Carina Nebula, Car OB1. Thanks to this census and high-resolution spectra from GES and the LiLIMaRlin library, we obtained a reliable distribution of rotational velocities for the O-star population in the GES footprint of Carina.

The census

The Gaia ESO Survey (**GES**) sample of early-type massive stars in Carina consists of 234 stars. The addition of brighter sources from the Galactic O-Star Spectroscopic Survey (**GOSSS**) and additional sources from the literature, allow us to create the most complete census of massive stars done so far in the region.

GES + GOSSS + GOSC + other sources

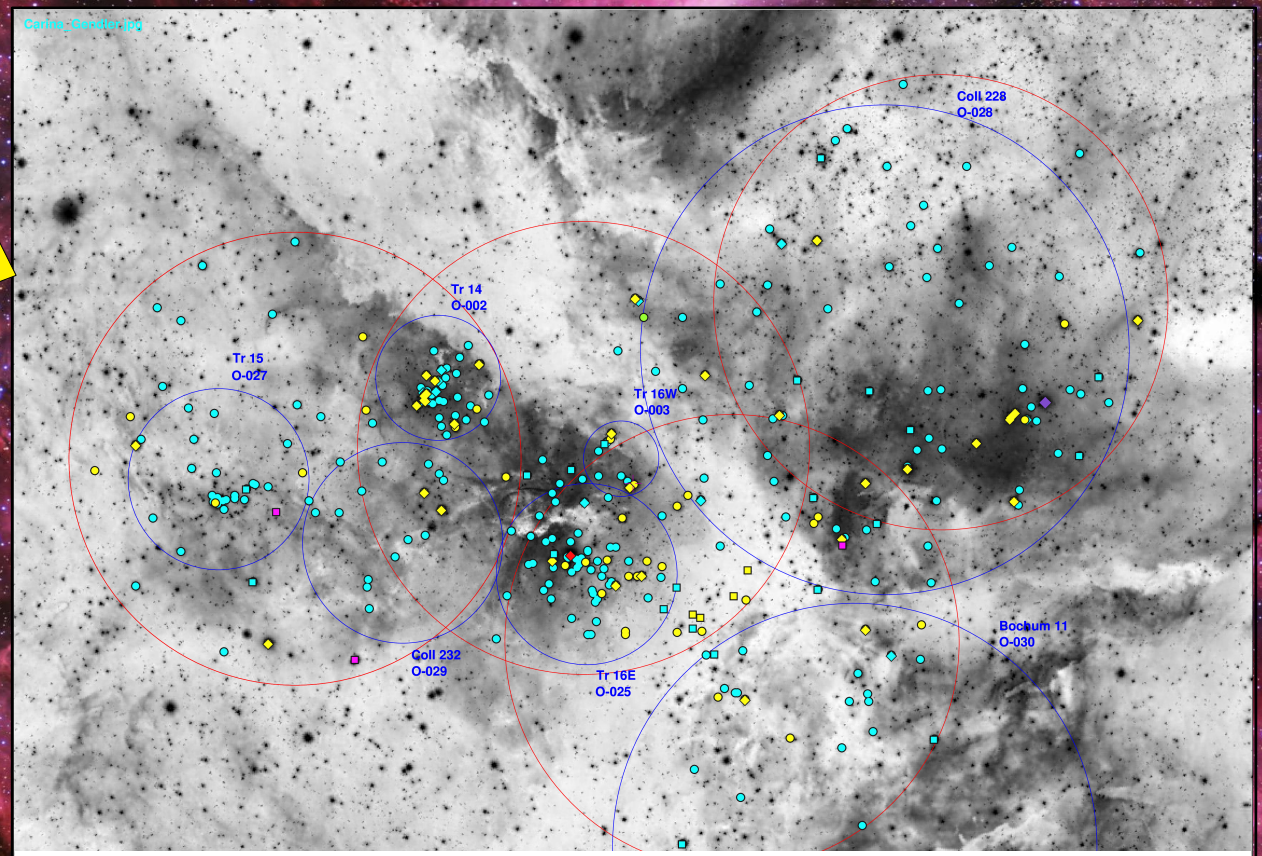

Fig. 1. Inverse image of the Great Carina Nebula by Robert Gendler and Stephane Guisard showing the location of the whole census of massive stars in the GES surveyed area presented in this work. Yellow and cian colors indicate O and B-type stars, respectively. Green, red, purple and pink colors have been used to represent the sdO, LBV, WR and RSG stars, respectively. Small filled-circles refer to the GES sample while rhombuses and squares refer to stars from GOSSS/LiLiMarlin and other works (Smith 2006a; Alexander et al. 2016; Preibisch et al. 2021) not present in GES, respectively. Red circles indicate the observing GES pointings while the blue ones indicate the Villafranca groups: O-002 (Trumpler 14), O-003 (Trumpler 16 W), O-025 (Trumpler 16 E), O-027 (Trumpler 15), O-028 (Collinder 228), O-029 (Collinder 232), and O-030 (Bochum 11). The V-shpaed extinction lane that dominates the appearance of the nebula is clearly seen crossing the image from top to bottom.

NOTE THAT ..

Massive OB stars include all O-types and those B2-types or earlier for dwarfs, B5-types or earlier for giants, and all B subtypes for supergiants (I or II luminosty classes). Red supergiants (RSG), Wolf-Rayet (WR) stars, and some B subtypes close to the OB-star limit (e.g. B2.5 V) are also included in the census for completeness.

Overall properties

The final census contains a total of **315 stars**, being 17 of them in the background and four in the foreground.

Of the 294 stellar systems in Car OB1, **74 are of O type, 214 are of non-supergiant B type and 6 are of WR or non-O supergiant (II to Ia) spectral class.**

Within the sample, we identified **18 spectroscopic binary systems with an O-star primary and another 17 with a B-star primary.**

The census

The observed CMD and completeness

O and B stars are separated in the CMD, with the O stars mostly above the average age 30 kK extinction track for R_{5495}= 4.5 and the B stars below it. **This is an indirect confirmation of the quality of the spectral classifications.**

The separation is not perfect but it is not expected to be for several reasons: B giants and supergiants (plus some early B + early B binaries) are expected to be above it and late O-dwarfs near the ZAMS below it.

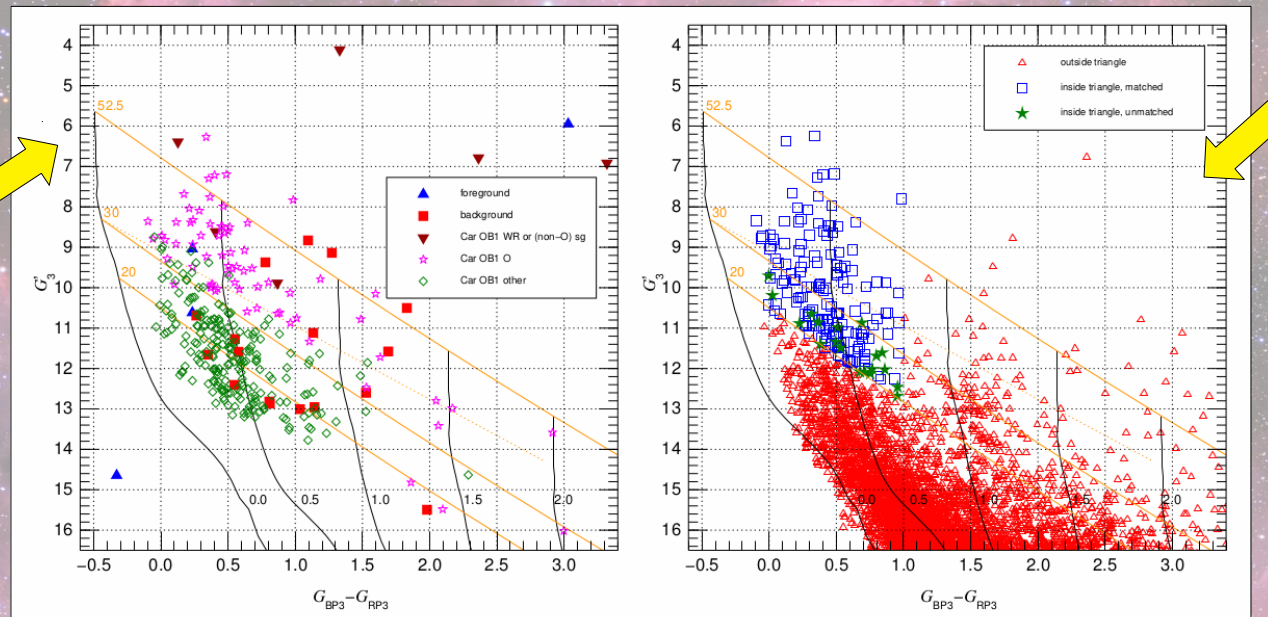

Fig. 2. *left* : *Gaia* EDR3 CMD for the stars with spectral types in this paper. Different symbols and colors are used to represent stars with parallaxes compatible with being (or otherwise assumed to be) in the foreground (4), in the background (17), or in Car OB1 (294). Of the Car OB1 stars, 6 are of Wolf-Rayet or non-O supergiant (II to Ia) spectral class, 74 are of O type, and 214 are of non-supergiant B type. Four of the Preibisch et al. (2021) stars are outside the frame towards the lower right due to their high extinction. Black lines show the average main sequence at a distance of 2.35 kpc with no extinction and with values of $E(4405-5495)$ of 0.5, 1.0, 1.5, and 2.0 (labelled) using the extinction law of Maíz Apellániz et al. (2014) with a value of R_{5495} of 4.5, which is typical of the region but with a large dispersion (Maíz Apellániz & Barbá 2018). Solid orange lines show the R_{5495} = 4.5 extinction tracks for average MS stars of $T_{\rm eff}$ of 52.5 kK, 30 kK, and 20 kK (labelled), respectively. The dotted orange line show the R_{5495} = 3.0 extinction track for $T_{\rm eff}$ = 30 kK. *Right* : Equivalent plot but for all *Gaia* EDR3 stars in the region of interest with corrected parallaxes that are compatible with the distance to Car OB1 and positive and with catalog values of $G_{BP3} - G_{RP3}$. The plotted objects are classified according to whether they are located inside or outside of the (quasi-)triangle defined by $G_{BP3} - G_{RP3}$ = 1.0 and the R_{5495} = 4.5 extinction track for average MS stars with $T_{\rm eff}$ = 20 kK. Stars inside the triangle are further divided into those matched with objects in the left panel (154) and those unmatched (19). Note that an additional three stars inside the triangle in the left panel (HD 93 129 Ab, CPD −59 2636 A,B, and ALS 19 740) plus η Car outside the triangle are not shown either because they are not included in *Gaia* EDR3 or have no parallaxes there.

In addition to that main sequence, a significant population of red stars is present.

We estimate that our sample is around 90% complete for low to moderate extinction O and early B systems.

Furthermore, the location of the 19 green stars, all of them below the 30 kK extinction track, suggests that those missing objects are likely early-B stars.

We are missing very few or even no low/moderate O-type systems in Car OB1 within our footprint in our sample. The 74 Car OB1 O- type systems in this paper are the largest nearly complete sample of objects of that spectral type in any part of a Galactic OB association

The distribution of rotational velocities

GES + LiLiMaRlin High-Res spectra

Line-broadening characterization

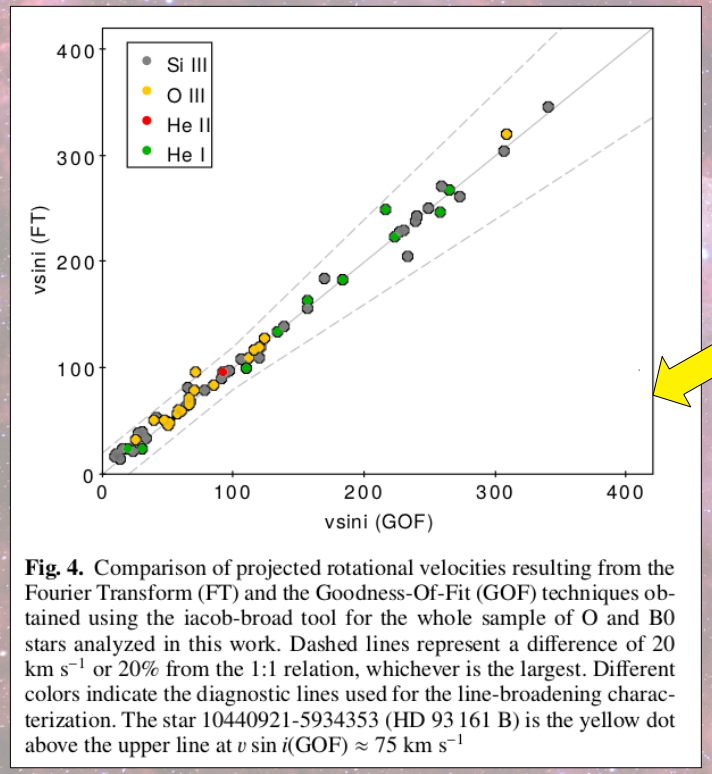

Fig. 4. Comparison of projected rotational velocities resulting from the Fourier Transform (FT) and the Goodness-Of-Fit (GOF) techniques obtained using the iacob-broad tool for the whole sample of O and B0 stars analyzed in this work. Dashed lines represent a difference of 20 km s^{-1} or 20% from the 1:1 relation, whichever is the largest. Different colors indicate the diagnostic lines used for the line-broadening characterization. The star 10440921-5934353 (HD 93 161 B) is the yellow dot above the upper line at $v \sin i$(GOF) ≈ 75 km s^{-1}

In order to obtain a reliable distribution of rotational velocities for the O population in Carina, **high-resolution spectroscopy** for the maximum number of O stars in the census **is required to reach low rotational velocities and better disentangle the macroturbulence broadening.**

We used **iacob-broad**, a tool that combines ***Fourier Transform*** **and the** ***Goodnest-of-fit*** **methods** to derive rotational velocities for the sample of O and B0 stars of our census for which high-resolution spectra is available.

Si III 4552 and O III 5592 diagnostic lines were prioritized. In case none of them are present, we use the nebular free or weakly contaminated **He I lines** (He I 4387, 4471, 4713). Only when the He I lines are weak or too noisy, we then rely on He II 4542.

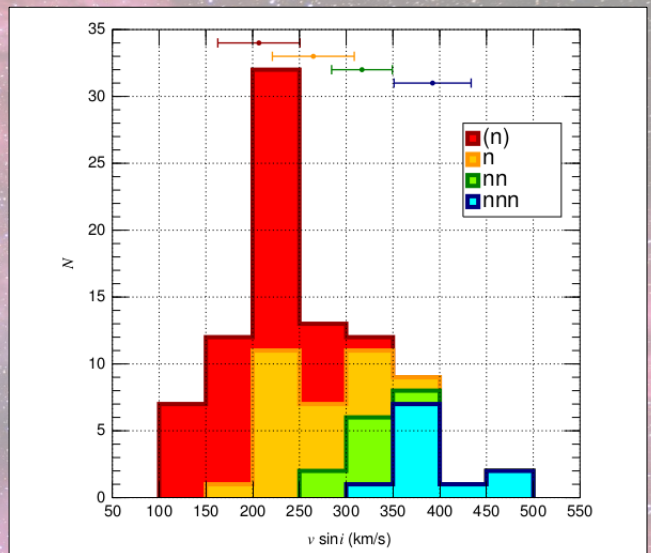

Fig. 5. $v \sin i$ histogram of those OB stars with any rotation index in their spectral classification. Broadening is denoted by (n), n, nn and nnn indexes, going the series from somewhat to more and even more broadened lines. Points and horizontal lines on the top of the figure indicate the mean $v \sin i$ value for each rotating group and their corresponding uncertainties, respectively.

We find a **correlation between rotational index** from spectral classifications (using the MGB tool) **and derived projected rotational velocities**, confirming the higher rotation index the higher rotational velocity.

The distribution of rotational velocities

vsini distribution for the O-star population of Car OB1

We obtained the distribution of rotational velocities for a sample of **38 O stars**, 22 of them observed by GES and 16 observed by LiLiMaRlin-OWN. This number represents a **68% fraction of the total known population of 56 single O-type stars present in our census**, providing us with a representative distribution of rotational velocities for the O-star population in Carina.

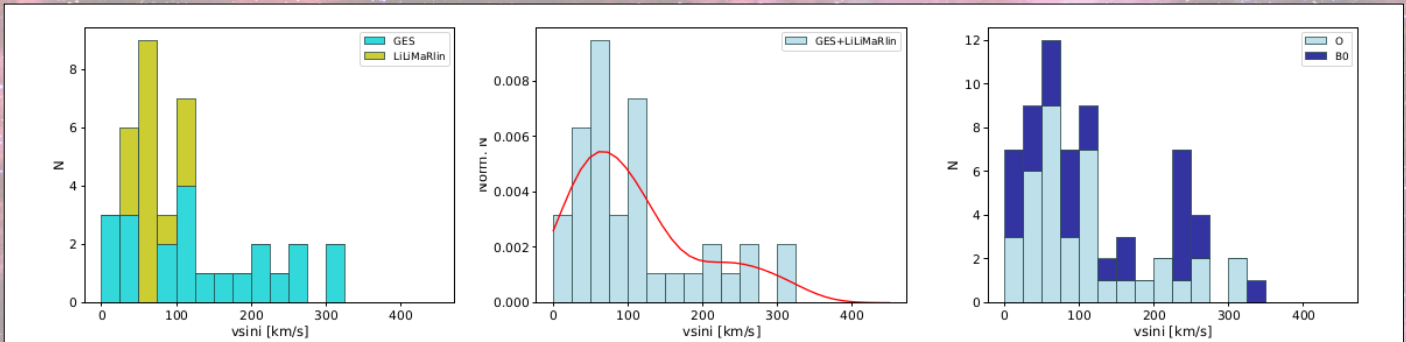

Fig. 6. *Left*: Distribution of rotational velocities for the sample of 22 and 16 O-type stars in Carina from GES (turquoise color) and LiLiMaRlin (green color) catalogs, respectively. *Middle*: Normalized distribution for the full sample of O-type stars. The red line represents a kernel density estimation using Gaussian kernels. *Right*: Distribution for the full sample of O-type stars (light blue) including B0-type stars identified in the GES catalog (dark blue).

We found the low velocity peak at 60 km s^{-1} and a tail of fast rotators above 200 km s^{-1}, as expected from previous results in other surveys. We observe an evident lack of stars in the 75-100 km s^{-1} bin, but it is highly attenuated when adding the sample of B0 stars.

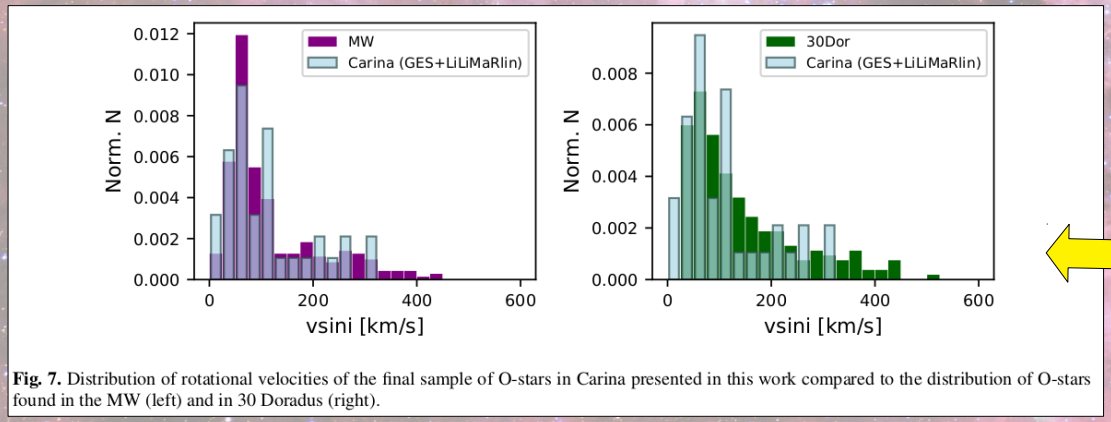

Fig. 7. Distribution of rotational velocities of the final sample of O-stars in Carina presented in this work compared to the distribution of O-stars found in the MW (left) and in 30 Doradus (right).

The distribution is very similar for both, a general sample of Galactic O stars and those in 30 Doradus, showing a bimodal structure although a shorter tail of fast rotators is found in Carina. However, it can be explained by considering the relative small size of our sample and the young age of Carina, which may imply insufficient time for binary interactions to produce such an extended tail of fast rotators.

For any questions, please contact ***sara.rb@ua.es***

The complete study will be published soon (*in prep.*):

Gaia-ESO Survey: Massive stars in the Carina Nebula
I. New census of OB stars and the distribution of rotational velocities for the O-star population

S. R. Berlanas, J. Maíz Apellániz, A. Herrero , L. Mahy , R. Blomme, I. Negueruela, R. Dorda, F. Comerón, F. Martins, E. Gosset, M. Pantaleoni González, J. A. Molina Lera, A. Sota & GES Survey Buldiers

SRB acknowledges financial support from the Spanish Government under grant PGC2018-093741-B-C21 (MICIU/AEI/FEDER, UE) and also by MCIN/AEI/10.13039/501100011033 (contract FJC 2020-045785-I) and NextGeneration EU/PRTR and MIU (UNI/551/2021) trough grant Margarita Salas-ULL. JMA acknowledges support from the Spanish Government Ministerio de Ciencia e Innovación and Agencia Estatal de Investigación (10.130 39/501 100 011 033) through grant PGC2018-95 049-B-C22. AH thanks support by the Spanish MCI trough grant PGC-2018-0913741-B-C22 and the Severo Ochoa Program trough CEX2019-000920-S